Available online at www.sciencedirect.com

ScienceDirect

Nuclear Physics A 1014 (2021) 122258

NUCLEAR PHYSICS A

www.elsevier.com/locate/nuclphysa

Remarks on *volume* fluctuations in fixed-target heavy-ion experiments

M. Mackowiak-Pawlowska [a], M. Naskręt [b,*], M. Gazdzicki [c,d]

[a] *Faculty of Physics, Warsaw University of Technology, Warsaw, Poland*
[b] *University of Wroclaw, Wrocław, Poland*
[c] *Geothe-University Frankfurt am Main, Germany*
[d] *Jan Kochanowski University, Kielce, Poland*

Received 11 March 2021; received in revised form 16 June 2021; accepted 18 June 2021
Available online 24 June 2021

Abstract

Experimental and theoretical studies of fluctuations in nucleus-nucleus interactions at high energies have started to play a major role in understanding of the concept of strong interactions. The elaborated procedures have been developed to disentangle different processes happening during nucleus-nucleus collisions. The fluctuations caused by a variation of the number of nucleons which participated in a collision are frequently considered the unwanted one. The methods to reduce the impact of these fluctuations in fixed-target experiments are reviewed and tested. They can be of key importance in the following ongoing fixed-target heavy-ion experiments: NA61/SHINE at the CERN SPS, STAR-FXT at the BNL RHIC, BMN at JINR Nuclotron, HADES at the GSI SIS18 and in future experiments such as NA60+ at the CERN SPS, CBM at the FAIR SIS100, JHITS at J-PARC-HI MR.

Keywords: Heavy-ion collisions; Fluctuations; Fixed-target experiments

1. Introduction

Measuring event-by-event fluctuations is the focus of numerous experimental programmes on nucleus-nucleus collisions at high energies. Nowadays, the leading motivation is the possibility

* Corresponding author.
E-mail address: majam@cern.ch (M. Mackowiak-Pawlowska).

https://doi.org/10.1016/j.nuclphysa.2021.122258

to discover the critical point of strongly interacting matter and a need to understand how the onset of deconfinement influences event-by-event fluctuations. The recent reviews can be found in Refs. [1–4].

Fluctuations in high energy collisions are significantly influenced by fluctuations in the amount of matter (*volume*) and energy involved in a collision, as well as global and local conservation laws. These fluctuations are unwanted effects in the search for the critical point and the study of the onset of deconfinement.

In this paper methods to reduce the influence of the *volume* fluctuations in fixed target experiments are reviewed and tested. They can be of key importance in the following ongoing fixed-target heavy-ion experiments: NA61/SHINE [5] at the CERN SPS, STAR-FXT [6] at the BNL RHIC, BMN [7] at the JINR Nuclotron, HADES [8] at the GSI SIS18, and in the future experiments such as NA60+ [9] at the CERN SPS, CBM [10] at the FAIR SIS100, JHITS [11] at J-PARC-HI MR.

The paper is organised as follows: Section 2 introduces the reference model - the Wounded Nucleon Model (WNM) [12] - used here to test the influence of the *volume* fluctuations. This section also introduces extensive, intensive and strongly intensive measures of fluctuations [13, 14] and their *volume* dependence within WNM. The main features of typical fixed-target and collider experiments with respect to fluctuation measurements and the *volume* fluctuations are summarised in Sec. 3. Two methods used to reduce the effect of the *volume* fluctuations in fixed-target experiments are introduced and compared using WNM in Sec. 4. The summary concludes the paper.

2. Wounded Nucleon Model, extensive and intensive quantities

Using the Wounded Nucleon Model [12] is probably the simplest way to introduce fluctuations of the amount of matter involved in a collision and their impact on the fluctuations of produced particles. The model was proposed in 1976 as the late child of the S-matrix period [15]. It assumes that particle production in nucleon-nucleon and nucleus-nucleus collisions is an incoherent superposition of particle production from wounded nucleons. The wounded nucleons are the ones which interacted inelastically and which number is calculated using straight line trajectories of nucleons. The properties of wounded nucleons are independent of the size of the colliding nuclei, e.g., they are the same in p+p and Pb+Pb collisions at the same collision energy per nucleon. Within WNM, the number of wounded nucleons plays the role of *volume*. These assumptions are graphically illustrated in Fig. 1.

We note that this simple model fails to describe many properties of experimental data. The WNM was selected here as the only focus of the paper is to study effects related to *volume* fluctuations and this is the simplest model which allows to factorise them from collision dynamics.

The extensive quantity is proportional to the system *volume*, which in the WNM is represented by W. It consists of target wounded nucleons, W_T as well as of projectile wounded nucleons, W_P. Let an event variable $\mathcal{A}$ be a sum of corresponding random variables a_i for wounded nucleons:

$$\mathcal{A} = a_1 + a_2 \cdots + a_W \ . \tag{1}$$

For example, a_i can be particle multiplicity produced by i-th wounded nucleon n_i and then $\mathcal{A}$ is collision multiplicity, $N = \sum_{i=1}^{W} n_i$.

The k-th order moment of the probability distribution of $\mathcal{A}$, $P(\mathcal{A})$, is defined as

$$\langle \mathcal{A}^k \rangle = \sum_{\mathcal{A}} \mathcal{A}^k P(\mathcal{A}). \tag{2}$$

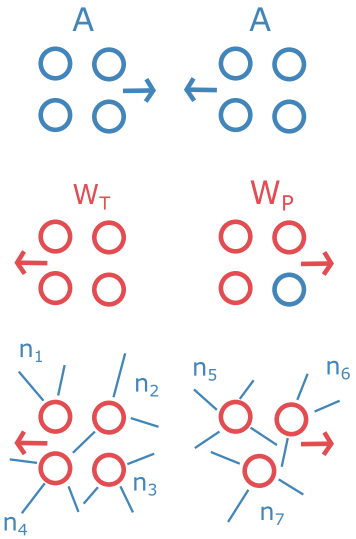

Fig. 1. The sketch of particle production process in nucleus-nucleus collisions according to the Wounded Nucleon Model [12]. Projectile and target nuclei with nuclear mass number A_P and A_T (here $A = A_P = A_T = 4$) collide. W_T (here $W_T = 4$) target wounded nucleons and W_P (here $W_P = 3$) projectile wounded nucleons produce N particles, where N is given by the sum over all wounded nucleons of particle multiplicities n_i from a single wounded nucleon, $N = \sum_{i=1}^{7} n_i$.

Then the extensive quantities which correspond to $\mathcal{A}$ are cumulants of $\mathcal{A}$ by

$$\kappa_1[\mathcal{A}] = \langle \mathcal{A} \rangle, \tag{3}$$

$$\kappa_2[\mathcal{A}] = \langle \delta\mathcal{A}^2 \rangle = Var[\mathcal{A}], \tag{4}$$

$$\kappa_3[\mathcal{A}] = \langle \delta\mathcal{A}^3 \rangle, \tag{5}$$

$$\kappa_4[\mathcal{A}] = \langle \delta\mathcal{A}^4 \rangle - 3\langle \delta\mathcal{A}^2 \rangle \tag{6}$$

$$\dots ,$$

where $\langle (\delta\mathcal{A})^k \rangle = \langle (\mathcal{A} - \langle \mathcal{A} \rangle)^k \rangle$. The first and the second cumulants are referred to as the mean and variance of $\mathcal{A}$, respectively. The third and fourth cumulants are related to skewness, $S = \kappa_3/\kappa_2^{3/2}$ and kurtosis, $\kappa = \kappa_4/\kappa_2^2$, respectively. By definition, cumulants are proportional to W.

An intensive quantity is the quantity which is independent of *volume*. Clearly, the ratio of two extensive quantities is the intensive quantity. For example, the ratio of the two first cumulants referred to as scaled variance is an intensive quantity:

$$\omega[\mathcal{A}] = \kappa_2[\mathcal{A}]/\kappa_1[\mathcal{A}]. \tag{7}$$

Other frequently used intensive quantities which involve third and fourth moments of $\mathcal{A}$ are:

$$\kappa_3[\mathcal{A}]/\kappa_2[\mathcal{A}], \quad \kappa_4[\mathcal{A}]/\kappa_2[\mathcal{A}], \tag{8}$$

sometimes denoted as $S\sigma$ and $\kappa\sigma^2$, respectively. For any probability distribution $P(W)$, the scaled variance calculated within the WNM reads [14]:

$$\omega[\mathcal{A}] = \omega[\mathcal{A}]_{fixed} + \langle \mathcal{A} \rangle / \langle W \rangle \cdot \omega[W] \,, \tag{9}$$

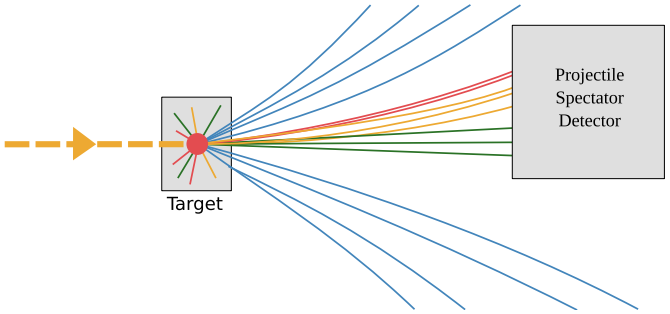

Fig. 2. The sketch of a nucleus-nucleus collision as seen by a fixed-target experiment. The incoming beam particle (marked with thick dashed orange line ▪ ▪ ▪) interacts inelastically with a target nucleus. Projectile spectators: protons (—), neutrons (—) and fragments (—) propagate to the forward calorimeter. Newly produced hadrons' trajectories (—) are bent and hadrons propagate to tracking detectors. (For interpretation of the colours in the figure(s), the reader is referred to the web version of this article.)

where $\omega[N]_{fixed}$ stands for the scaled variance at any fixed number of wounded nucleons were $W = W_P + W_T$. In this situation there is no volume fluctuation by construction. The first component of Eq. (9) is considered the wanted one and it is independent of the *volume* fluctuations. However, the second component is unwanted and it is proportional to the scaled variance of the W distribution. Corresponding expressions for higher order moments are given in Ref. [16].

It is worth noting that similar relations are valid within Statistical Models of an Ideal Boltzmann gas within the Grand Canonical Ensemble SM(IB-GCE) [14]. Then, in the equations above, the number of wounded nucleons W should be replaced by the gas volume V.

3. Fixed-target versus collider experiments

Typically, fixed-target experiments - like NA49 and NA61/SHINE at the CERN SPS - cover mostly the forward hemisphere in the centre-of-mass system. An advantage of the fixed-target geometry is that it allows to select collisions using the measured energy of spectators from the beam nucleus independently from measurements of the produced particles, see Fig. 2 for illustration. This selection is referred to as *centrality* selection. It is important to note that the measurement of target spectators is usually impossible as most of them are fully stopped inside the target material.

On the other hand, a typical collider experiment – like STAR at BNL RHIC and ALICE at CERN LHC – has practically energy-independent rapidity acceptance, but without the low transverse momentum region. The track density in the detector increases only moderately with the collision energy. However, *left* and *right* spectator regions are only partly accessible to measurements and the collision selection is usually based on the multiplicity of produced particles, see Fig. 3 for illustration. Thus, quantities used to select events and study the properties of particle production are correlated by the physics of particle production [18]. This fact complicates the interpretation of the results. For details on centrality selection in collider experiments and its impact on fluctuation quantities see Refs. [2,19–21].

4. Two methods to reduce *volume* fluctuations

In this section, the following two popular methods to reduce the impact of the *volume* fluctuations – the unwanted component in Eq. (9), are discussed:

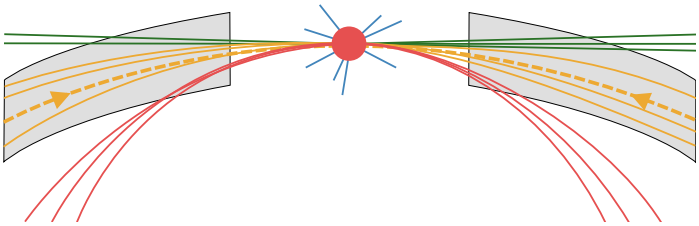

Fig. 3. The sketch of a nucleus-nucleus collision as seen by collider experiments. The incoming beam particles (marked with thick dashed orange line ▪ ▪ ▪) interact inelastically with each other. Measurements of *left* and *right* spectators are possible under the same experimental conditions. However, only free nucleon spectators (▬ and ▬) – in central collisions about 50% of all nucleons [17] – can be measured. Fragments (▬) follow approximately the beam trajectories and they are difficult to measure. Newly produced hadrons (▬) propagate to other detectors.

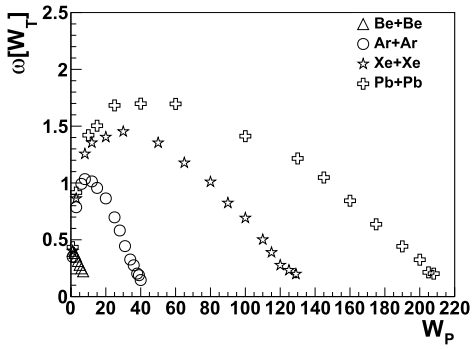

Fig. 4. Scaled variance of the distribution of the number of target wounded nucleons W_T as a function of the number of projectile wounded nucleons W_P calculated within the HIJING [22] implementation of the Wounded Nucleon Model [12]. The results for $^{7}\mathrm{Be} + {}^{7}\mathrm{Be}$, $^{40}\mathrm{Ar} + {}^{40}\mathrm{Ar}$, $^{129}\mathrm{Xe} + {}^{129}\mathrm{Xe}$ and $^{208}\mathrm{Pb} + {}^{208}\mathrm{Pb}$ collisions at 19A GeV/c are presented.

(i) selection of the most *central* collisions,
(ii) use of strongly intensive quantities.

4.1. *The selection of the most* central *collisions*

To limit the unwanted component in fixed-target experiments, collisions with the smallest number of projectile spectators are selected. This is done with collision-by-collision measurement of a forward energy that is predominantly the energy of projectile spectators, see Fig. 2. In order to simplify, let us assume that only collisions with zero number of projectile spectators were selected and thus $W_P = A_P$, where A_P is the nuclear mass number of projectile nucleus. Then, it appears that for collisions of sufficiently large nuclei of similar nuclear mass number, the number of target wounded nucleons is also fixed. This is demonstrated in Fig. 4 where results obtained within the HIJING [22] implementation of the Wounded Nucleon Model [12] are shown. These results agree with the predictions of the HSD and UrQMD models [23]. Thus, the total number of wounded nucleons $W = W_P + W_T$ is approximately fixed for very *central* collisions and its scaled variance is close to zero so the unwanted component in Eq. (9) is eliminated.

4.2. The use of strongly intensive quantities

Since even for the most *central* collisions the *volume* fluctuations cannot be fully eliminated, it is important to minimise their effect further by defining suitable fluctuation measures. It appears that for the WNM and the SM(IB-GCE) models [13,14,24] fluctuation measures independent of the *volume* fluctuations can be constructed using moments of the distribution of two extensive quantities.

As the simplest example, let us consider multiplicities of two different types of hadrons, $\mathcal{A}$ and $\mathcal{B}$. Their mean multiplicities are proportional to W:

$$\langle \mathcal{A} \rangle \sim W \ , \quad \langle \mathcal{B} \rangle \sim W. \tag{10}$$

Obviously the ratio of mean multiplicities is independent of W. Moreover, the ratio $\langle \mathcal{A} \rangle / \langle \mathcal{B} \rangle$ is independent of $P(W)$, where $P(W)$ is the probability distribution of W for a selected set of collisions. The quantities which have the latter property are called strongly intensive quantities [14]. Such quantities are useful in experimental studies of fluctuations in A+A collisions as they eliminate the influence of a usually poorly known distribution of W.

More generally, $\mathcal{A}$ and $\mathcal{B}$ can be any extensive event quantities such as the sum of transverse momenta, the net charge or the multiplicity of particles of a given type. The scaled variance of $\mathcal{A}$ and $\mathcal{B}$ and the mixed second moment $\langle \mathcal{A} \cdot \mathcal{B} \rangle$ calculated within the WNM [14] read:

$$\omega[\mathcal{A}] = \omega^*[\mathcal{A}] + \langle \mathcal{A} \rangle / \langle W \rangle \cdot \omega[W] \ , \tag{11}$$

$$\omega[\mathcal{B}] = \omega^*[\mathcal{B}] + \langle \mathcal{B} \rangle / \langle W \rangle \cdot \omega[W] \ , \tag{12}$$

$$\langle \mathcal{A} \cdot \mathcal{B} \rangle = \langle \mathcal{A} \cdot \mathcal{B} \rangle^* \langle W \rangle + \langle \mathcal{A} \rangle \langle \mathcal{B} \rangle \langle W \rangle^2 \cdot (\langle W^2 \rangle - \langle W \rangle) \ , \tag{13}$$

where the quantities denoted by * are quantities calculated at a fixed *volume*.

From Eqs. (11)-(13) it follows [14,25] that

$$\Delta[\mathcal{A}, \mathcal{B}] \ = \ \frac{1}{C_\Delta} \Big[\langle \mathcal{B} \rangle \, \omega[\mathcal{A}] \ - \ \langle \mathcal{A} \rangle \, \omega[\mathcal{B}] \Big] \tag{14}$$

and

$$\Sigma[\mathcal{A}, \mathcal{B}] \ = \ \frac{1}{C_\Sigma} \Big[\langle \mathcal{B} \rangle \, \omega[\mathcal{A}] \ + \ \langle \mathcal{A} \rangle \, \omega[\mathcal{B}] \ - \ 2 \, (\langle \mathcal{A} \cdot \mathcal{B} \rangle - \langle \mathcal{A} \rangle \langle \mathcal{B} \rangle) \Big] \tag{15}$$

are independent of $P(W)$ in the WNM. Here, the normalisation factors C_Δ and C_Σ are required to be proportional to the first moments of any extensive quantity. In Ref. [25] a specific choice of the C_Δ and C_Σ normalisation factors was proposed which makes the quantities $\Delta[\mathcal{A}, \mathcal{B}]$ and $\Sigma[\mathcal{A}, \mathcal{B}]$ dimensionless and leads to $\Delta[\mathcal{A}, \mathcal{B}] = \Sigma[\mathcal{A}, \mathcal{B}] = 1$ in the independent particle model (IPM) [25]. This normalisation is referred to as the IPM normalisation and it is used here.

Thus, $\Delta[\mathcal{A}, \mathcal{B}]$ and $\Sigma[\mathcal{A}, \mathcal{B}]$ are strongly intensive quantities which measure fluctuations of $\mathcal{A}$ and $\mathcal{B}$, i.e. they are sensitive to second moments of the distributions of the quantities $\mathcal{A}$ and $\mathcal{B}$. The results on $\Delta[\mathcal{A}, \mathcal{B}]$ and $\Sigma[\mathcal{A}, \mathcal{B}]$ are referred to as the results on $\mathcal{A} - \mathcal{B}$ fluctuations, e.g., transverse momentum - multiplicity fluctuations. The analogous quantities called strongly intensive cumulants allow to measure fluctuations of higher order moments [24]. The first four are defined as:

$$\kappa_1^*[\mathcal{A}, \mathcal{B}] = \frac{\langle \mathcal{A} \rangle}{\langle \mathcal{B} \rangle}$$

$$\kappa_2^*[\mathcal{A}, \mathcal{B}] = \frac{\langle \mathcal{A}^2 \rangle}{\langle \mathcal{B} \rangle} - \frac{\langle \mathcal{A} \rangle \langle \mathcal{A} \cdot \mathcal{B} \rangle}{\langle \mathcal{B} \rangle^2}$$

$$\kappa_3^*[\mathcal{A},\mathcal{B}] = \frac{\langle \mathcal{A}^3\rangle}{\langle \mathcal{B}\rangle} - \frac{2\langle \mathcal{A}^2\rangle\langle \mathcal{A}\cdot\mathcal{B}\rangle + \langle \mathcal{A}\rangle\langle \mathcal{A}^2\cdot\mathcal{B}\rangle}{\langle \mathcal{B}\rangle^2} + \frac{2\langle \mathcal{A}\rangle\langle \mathcal{A}\cdot\mathcal{B}\rangle^2}{\langle \mathcal{B}\rangle^3} \tag{16}$$

$$\kappa_4^*[\mathcal{A},\mathcal{B}] = \frac{\langle \mathcal{A}^4\rangle}{\langle \mathcal{B}\rangle} - \frac{3\langle \mathcal{A}^3\rangle\langle \mathcal{A}\cdot\mathcal{B}\rangle + \langle \mathcal{A}\rangle\langle \mathcal{A}^3\cdot\mathcal{B}\rangle}{\langle \mathcal{B}^2\rangle} - \frac{3\langle \mathcal{A}^2\rangle\langle \mathcal{A}^2\cdot\mathcal{B}\rangle}{\langle \mathcal{B}^2\rangle} + \frac{6\langle \mathcal{A}^2\rangle\langle \mathcal{A}\cdot\mathcal{B}\rangle^2 + 6\langle \mathcal{A}\rangle\langle \mathcal{A}^2\cdot\mathcal{B}\rangle\langle \mathcal{A}\cdot\mathcal{B}\rangle}{\langle \mathcal{B}^3\rangle} - \frac{6\langle \mathcal{A}\rangle\langle \mathcal{A}\cdot\mathcal{B}\rangle^3}{\langle \mathcal{B}^4\rangle}$$

Because of their construction, strongly intensive measures of fluctuations require two extensive quantities. This, in general, hampers a straight-forward interpretation of the experimental results. However, under certain conditions the Δ quantity can be used to obtain the scaled variance of the extensive quantity $\mathcal{A}$ separately.

Let $\mathcal{A}$ be an extensive quantity, e.g., selected for its sensitivity to critical fluctuations. Then choose a quantity $\mathcal{B}$ such that $\mathcal{B} \sim W$ and denote it as $\mathcal{B}_{fixed}$. It is easy to show [1] that the strongly intensive measures $\Delta_{\mathcal{B}}[\mathcal{A},\mathcal{B}]$ and $\Sigma_{\mathcal{B}}[\mathcal{A},\mathcal{B}]$ (equal to $\Delta[\mathcal{A},\mathcal{B}]$ and $\Sigma_{\mathcal{B}}[\mathcal{A},\mathcal{B}]$ with the normalisation $C_\Delta = \langle \mathcal{B}\rangle \sim \langle W\rangle$) obey the relation:

$$\Delta_{\mathcal{B}}[\mathcal{A},\mathcal{B}] = \Sigma_{\mathcal{B}}[\mathcal{A},\mathcal{B}] = \omega^*[\mathcal{A}]\,. \tag{17}$$

Thus, $\Delta_{\mathcal{B}}[\mathcal{A},\mathcal{B}]$ is equal to the scaled variance $\omega[\mathcal{A}]$ for a fixed number of wounded nucleons (see Eq. (11)). Similar relations can be found for strongly intensive cumulants of any order:

$$\frac{\kappa_l^*}{\kappa_k^*}[\mathcal{A},\mathcal{B}_{fixed}] = \frac{\kappa_l[\mathcal{A}]}{\kappa_k[\mathcal{B}]}\,, \tag{18}$$

where l and k denote cumulants' orders and $l \neq k$. In the derivation of Eqs. (17) and (18) one assumes the validity of Eq. (11) which needs to be investigated case-by-case.

5. Numerical tests

Numerical tests of the methods to reduce the *volume* fluctuations introduced above are presented in this section. The simulations were performed using the HIJING [22] implementation of the Wounded Nucleon Model:

(i) ^{40}Ar+^{40}Ar collisions at 150A GeV/c were generated. This reaction closely corresponds to data recorded by NA61/SHINE at the CERN SPS [26].
(ii) for each collision, number of projectile and target wounded nucleons and impact parameter b are stored.
(iii) number of particles n produced by a given wounded nucleon is drawn from the binomial distribution with maximum equal to 2 and probability equal to 0.5:

$$P(n) = \binom{2}{n} 0.5^2. \tag{19}$$

Moments of this distribution are: $\langle n\rangle = 1$, $\omega[n] = 0.5$, $\kappa_3[n]/\kappa_2[n] = 0$ and $\kappa_4[n]/\kappa_2[n] = -0.5$.

5.1. *Selecting the most* central *collisions*

Fig. 5 shows the dependence of $\omega[N]$, $\kappa_3[N]/\kappa_2[N]$ and $\kappa_4[N]/\kappa_2[N]$ on the ratio W_P/A_P. The quantities approach the corresponding value for a fixed number of wounded nucleons with

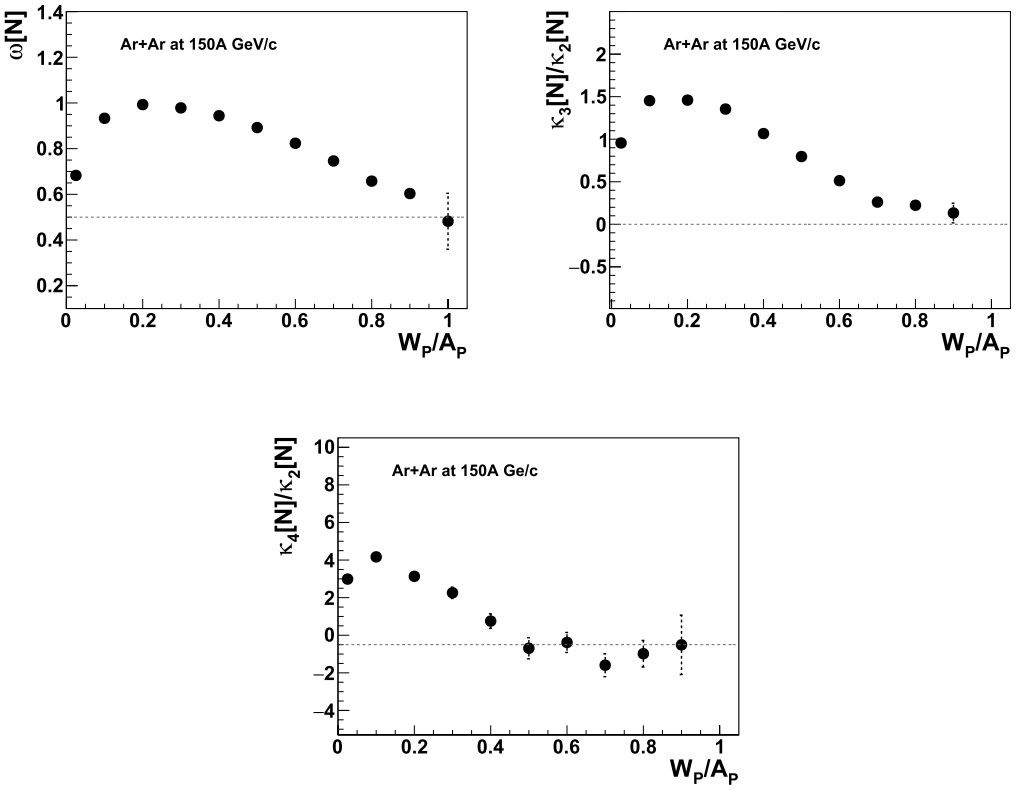

Fig. 5. The dependence of $\omega[N]$, $\kappa_3[N]/\kappa_2[N]$ and $\kappa_4[N]/\kappa_2[N]$ on the ratio W_P/A_P within the Wounded Nucleon Model with input defined in Sec. 5. The reference values for any fixed number of wounded nucleons $W = const$ are shown by dashed lines. The calculations were performed for ^{40}Ar+^{40}Ar collisions at 150A GeV/c.

$W_P/A_P \to 0$. It is important to note that only $\approx 0.0007\%$ of all inelastic collisions have $W_P = A_P$.

It can be concluded that the selection of collisions with $W_P = A_P$ significantly reduces the effect of the *volume* fluctuations, however it is at the cost of reduction of event statistics. The remaining bias can be corrected for using a model-dependent correction [27,28]. The uncertainty of this correction will contribute to the systematic uncertainty of the final results.

5.2. Using strongly intensive quantities

Strongly intensive quantities were proposed with the aim to reduce the intrinsic limitation of the method based on the selection of *central* events which may lead to significant systematic and statistical uncertainties. Fig. 6 shows the dependence of intensive and strongly intensive quantities on the ratio of $\langle W_P \rangle / A_P$. Here, collisions were selected using collision impact parameter. As expected, strongly intensive quantities are equal or are close to the corresponding values for fixed W. Unlike strongly intensive quantities their intensive partners also shown in Fig. 6 significantly depend on the impact parameter selection. Thus, it can be concluded that strongly intensive quantities together with the impact parameter selection of collisions fully eliminates the effect of *volume* fluctuations. Unfortunately, this is not the solution of the problem. The collision

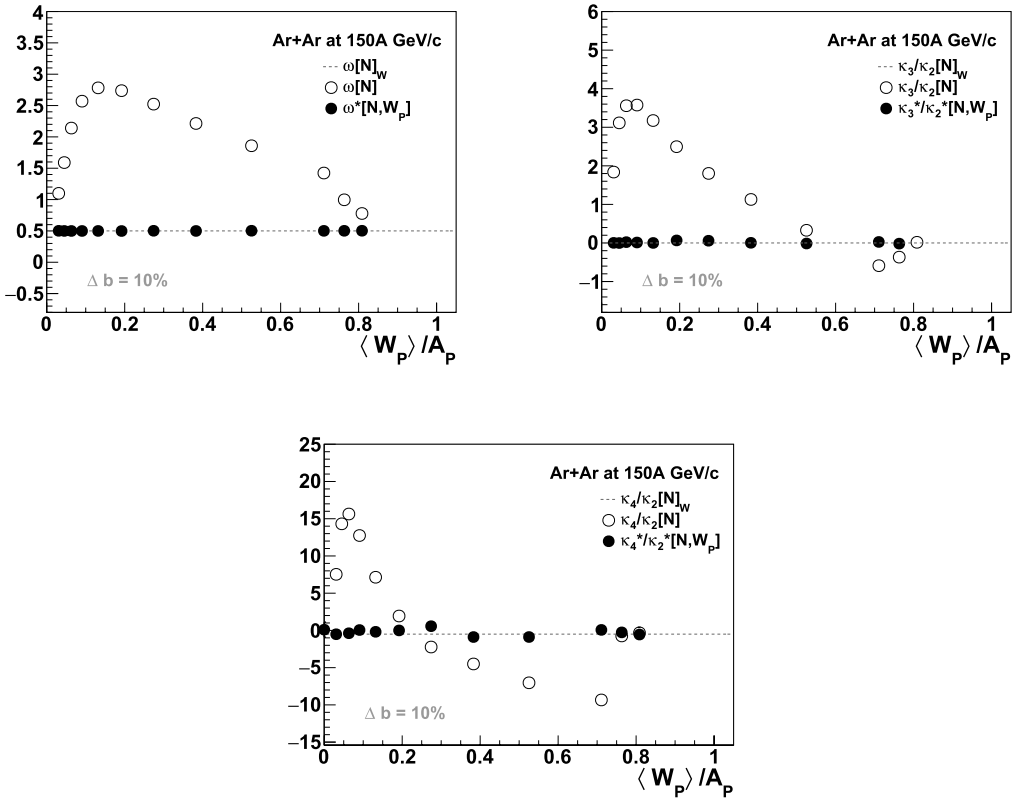

Fig. 6. The dependence of $\omega^*[N, W_P]$, $\kappa_3^*[N, W_P]/\kappa_2^*[N, W_P]$ and $\kappa_4^*[N, W_P]/\kappa_2^*[N, W_P]$ (full circles) as well as $\omega[N]$, $\kappa_3[N]/\kappa_2[N]$ and $\kappa_4[N]/\kappa_2[N]$ (open circles) on the ratio $\langle W_P \rangle / A_P$ within the Wounded Nucleon Model with input defined in Sec. 5. Results are obtained in bins of b. The most right two points which correspond to Δb equal to 5% and 1%. The values for $W = const$ are shown by dashed lines.

impact parameter is not a measurable quantity. So, calculating strongly intensive quantities for all inelastic collisions should be considered. Within the WNM and SM(IB-GCE) models, strongly intensive quantities for those collisions are equal to the corresponding quantities for fixed W. However, in general, the models are not valid in the full range of the impact parameter.

Consequently, the method of the event selection based on the number of projectile wounded nucleons needs to be used. The results calculated in bins of W_P are shown in Fig. 7. In this case strongly intensive quantities, in general, also deviate from the corresponding values for fixed W. They approach them only for the most *central* collisions, $W_P/A_P \to 1$. This is due to the introduced correlation when events are selected on the same quantity used to calculate strongly intensive quantities. This can be solved by defining strongly intensive quantities using two extensive quantities related to particle production properties. Particle multiplicity and transverse momentum [29,30] are the most popular examples of these quantities. However, when the goal is to obtain moments of multiplicity distribution for fixed W there is no significant advantage of using strongly intensive quantities. Similarly, intensive quantities have to be calculated in the most *central* collisions to approach the unbiased results.

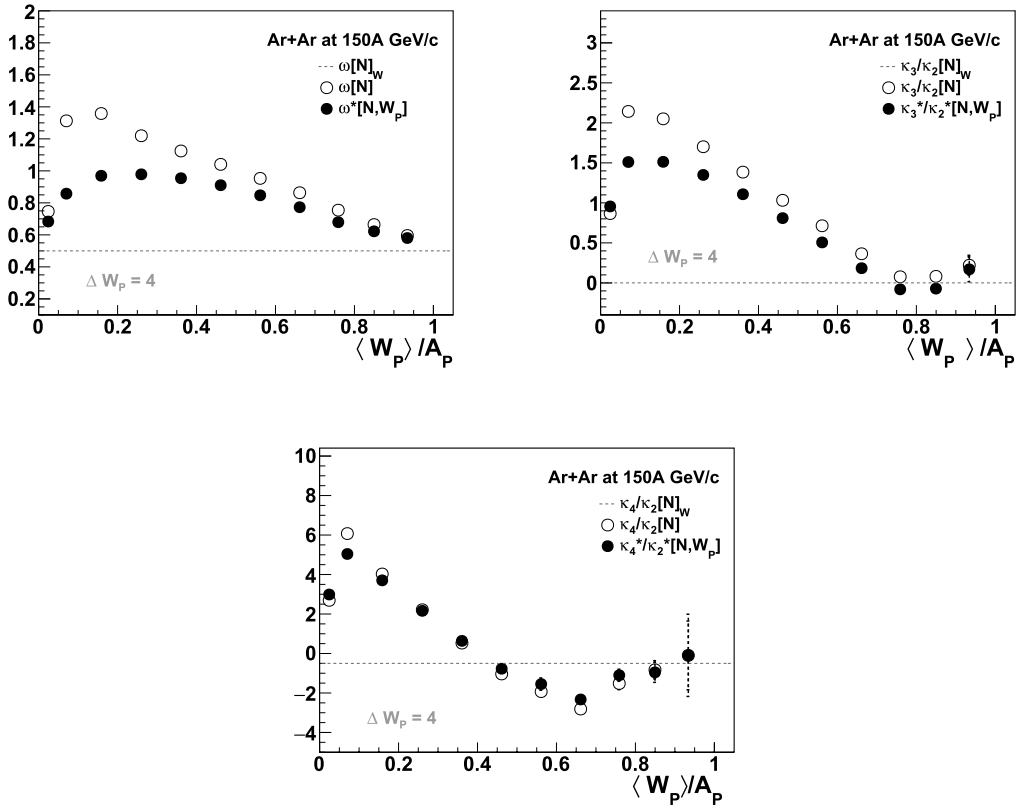

Fig. 7. The dependence of $\omega^*[N, W_P]$, $\kappa_3^*[N, W_P]/\kappa_2^*[N, W_P]$ and $\kappa_4^*[N, W_P]/\kappa_2^*[N, W_P]$ (full circles) as well as $\omega[N]$, $\kappa_3[N]/\kappa_2[N]$ and $\kappa_4[N]/\kappa_2[N]$ (open circles) on the ratio $\langle W_P \rangle / A_P$ within the Wounded Nucleon Model with input defined in Sec. 5. Results are obtained in bins of W_P. The values for $W = const$ are shown by dashed lines.

6. Summary

The paper addresses a currently important question of measuring event-by-event particle number fluctuations in nucleus-nucleus collisions unbiased by fluctuations of the collision *volume*. With this respect different properties of fixed-target and collider experiments are briefly summarised. Fixed-target experiments, unlike collider experiments, allow for measurements of all projectile spectators. This gives an opportunity for a least-biased selection of central collisions. Based on this property, two methods to reduce the influence of the *volume* fluctuations in fixed target experiments are reviewed and tested. Some of the limitations of *strongly intensive quantities* in these types of analysis are shown. The results indicate the need to select the most *central* collisions using the number of projectile spectators.

CRediT authorship contribution statement

M. Mackowiak-Pawlowska: Conceptualization, Formal analysis, Methodology, Software, Visualization, Writing – original draft, Writing – review & editing. **M. Naskręt:** Software, Visu-

alization, Writing – original draft, Writing – review & editing. **M. Gazdzicki:** Conceptualization, Writing – original draft, Writing – review & editing.

Declaration of competing interest

The authors declare that they have no known competing financial interests or personal relationships that could have appeared to influence the work reported in this paper.

Acknowledgements

The authors thank K. Grebieszkow and A. Seryakov as well as other participants of Ion and PSD meetings of the NA61/SHINE collaboration. This work was supported by the Polish National Science Centre grants 2016/21/D/ST2/01983, 2018/30/A/ST2/00226 and 2019/32/T/ST2/00432 as well as the German Research Foundation grant GA1480/8-1. MMP studies were also funded by IDUB-POB-FWEiTE-1 project granted by Warsaw University of Technology under the program Excellence Initiative: Research University (ID-UB).

References

[1] M. Gazdzicki, P. Seyboth, Search for critical behaviour of strongly interacting matter at the CERN super proton synchrotron, Acta Phys. Pol. B 47 (2016) 1201.
[2] X. Luo, N. Xu, Search for the QCD critical point with fluctuations of conserved quantities in relativistic heavy-ion collisions at RHIC: an overview, Nucl. Sci. Tech. 28 (8) (2017) 112.
[3] A. Bzdak, S. Esumi, V. Koch, J. Liao, M. Stephanov, N. Xu, Mapping the phases of quantum chromodynamics with beam energy scan, Phys. Rep. 853 (2020) 1–87.
[4] M. Gazdzicki, M. Gorenstein, P. Seyboth, Brief history of the search for critical structures in heavy-ion collisions, Acta Phys. Pol. B 4 (2020).
[5] N. Abgrall, et al., NA61/SHINE facility at the CERN SPS: beams and detector system, J. Instrum. 9 (2014) P06005.
[6] G. Odyniec, Beam energy scan program at RHIC (BES I and BES II) – probing QCD phase diagram with heavy-ion collisions, PoS CORFU2018 (2019) 151.
[7] V. Kekelidze, V. Kolesnikov, R. Lednicky, V. Matveev, A. Sorin, G. Trubnikov, Heavy ion collision experiments at NICA, PoS ICHEP2018 (2019) 493.
[8] G. Agakishiev, et al., The high-acceptance dielectron spectrometer HADES, Eur. Phys. J. A 41 (2009) 243–277.
[9] M. Agnello, et al., Study of hard and electromagnetic processes at CERN-SPS energies: an investigation of the high-$\mu_{\mathbf{B}}$ region of the QCD phase diagram with NA60+, arXiv:1812.07948 [nucl-ex], 2018.
[10] T. Ablyazimov, et al., Challenges in QCD matter physics – the scientific programme of the compressed baryonic matter experiment at FAIR, Eur. Phys. J. A 53 (3) (2017) 60.
[11] H. Sako, Studies of extremely dense matter in heavy-ion collisions at J-PARC, Nucl. Phys. A 982 (2019) 959–962.
[12] A. Bialas, M. Bleszynski, W. Czyz, Multiplicity distributions in nucleus-nucleus collisions at high-energies, Nucl. Phys. B 111 (1976) 461.
[13] M. Gazdzicki, S. Mrowczynski, A method to study 'equilibration' in nucleus-nucleus collisions, Z. Phys. C 54 (1992) 127.
[14] M. Gorenstein, M. Gazdzicki, Strongly intensive quantities, Phys. Rev. C 84 (2011) 014904.
[15] M. Gazdzicki, On the history of multi-particle production in high energy collisions, Acta Phys. Pol. B 43 (2012) 791.
[16] V. Begun, Participant number fluctuations for higher moments of a multiplicity distribution, arXiv:1606.05358 [nucl-th], 2016.
[17] H. Appelshäuser, et al., Spectator nucleons in Pb + Pb collisions at 158-A-GeV, Eur. Phys. J. A 2 (1998) 383–390.
[18] V.P. Konchakovski, M.I. Gorenstein, E.L. Bratkovskaya, Multiplicity fluctuations in Au + Au collisions at RHIC, Phys. Rev. C 76 (2007) 031901.
[19] X. Luo, J. Xu, B. Mohanty, N. Xu, Volume fluctuation and auto-correlation effects in the moment analysis of net-proton multiplicity distributions in heavy-ion collisions, J. Phys. G 40 (2013) 105104.

[20] P. Braun-Munzinger, A. Rustamov, J. Stachel, Bridging the gap between event-by-event fluctuation measurements and theory predictions in relativistic nuclear collisions, Nucl. Phys. A 960 (2017) 114–130.
[21] V. Skokov, B. Friman, K. Redlich, Volume fluctuations and higher order cumulants of the net baryon number, Phys. Rev. C 88 (2013) 034911.
[22] X.-N. Wang, M. Gyulassy, HIJING: a Monte Carlo model for multiple jet production in p p, p A and A A collisions, Phys. Rev. D 44 (1991) 3501–3516.
[23] V. Konchakovski, S. Haussler, M.I. Gorenstein, E. Bratkovskaya, M. Bleicher, H. Stoecker, Particle number fluctuations in high energy nucleus-nucleus collisions from microscopic transport approaches, Phys. Rev. C 73 (2006) 034902.
[24] E. Sangaline, Strongly intensive cumulants: fluctuation measures for systems with incompletely constrained volumes, arXiv:1505.00261 [nucl-th], 2015.
[25] M. Gazdzicki, M. Gorenstein, M. Mackowiak-Pawlowska, Normalization of strongly intensive quantities, Phys. Rev. C 88 (2) (2013) 024907.
[26] M. Mackowiak-Pawlowska, NA61/SHINE results on fluctuations and correlations at CERN SPS energies, in: 28th International Conference on Ultrarelativistic Nucleus-Nucleus Collisions, Feb. 2020.
[27] A. Aduszkiewicz, et al., Multiplicity and transverse momentum fluctuations in inelastic proton–proton interactions at the CERN Super Proton Synchrotron, Eur. Phys. J. C 76 (11) (2016) 635.
[28] A. Acharya, et al., Measurements of multiplicity fluctuations of identified hadrons in inelastic proton-proton interactions at the CERN Super Proton Synchrotron, Eur. Phys. J. C 81 (5) (2021) 384.
[29] T. Anticic, et al., Measurement of event-by-event transverse momentum and multiplicity fluctuations using strongly intensive measures $\Delta[P_T, N]$ and $\Sigma[P_T, N]$ in nucleus-nucleus collisions at the CERN Super Proton Synchrotron, Phys. Rev. C 92 (4) (2015) 044905.
[30] M.I. Gorenstein, K. Grebieszkow, Strongly intensive measures for transverse momentum and particle number fluctuations, Phys. Rev. C 89 (3) (2014) 034903.